

---

This is the **accepted version** of the article:

Hu, Minjie; Sardans i Galobart, Jordi; Yang, Xianyu; [et al.]. «Patterns and environmental drivers of greenhouse gas fluxes in the coastal wetlands of China : a systematic review and synthesis». *Environmental research*, Vol. 186 (July 2020), art. 109576. DOI 10.1016/j.envres.2020.109576

---

This version is available at <https://ddd.uab.cat/record/224226>

under the terms of the  license

# **Patterns and environmental drivers of greenhouse gas fluxes in the coastal wetlands of China: A systematic review and synthesis**

**Minjie Hu<sup>a, b\*</sup>, Jordi Sardans<sup>c, d</sup>, Xianyu Yang<sup>e</sup>, Josep Peñuelas<sup>c, d</sup>, Chuan Tong<sup>a\*</sup>**

<sup>a</sup> *Key Laboratory of Humid Sub-tropical Eco-geographical Process of Ministry of Education, Fujian Normal University, Fuzhou, 350007, Fujian, China*

<sup>b</sup> *College of the Environment and Ecology, Xiamen University, Xiamen, 361102, Fujian, China*

<sup>c</sup> *CSIC, Global Ecology CREAM-CSIC-UAB, Bellaterra, 08193 Barcelona, Catalonia, Spain*

<sup>d</sup> *CREAF, Cerdanyola del Vallès, 08193 Barcelona, Catalonia, Spain*

<sup>e</sup> *School of Ecological and Environmental Science, East China Normal University, Shanghai 200241, China*

**Abstract:**

Coastal wetlands play an increasingly important role in regulating greenhouse gas (GHG) fluxes and thus affecting climate change. However, the overall magnitude, trend, and environmental drivers of GHG fluxes in these wetlands of China remain uncertain. Herein, we synthesized data from 70 publications involving 187 field observations to identify patterns and drivers of GHG fluxes across coastal wetlands in China. Average methane (CH<sub>4</sub>), nitrous oxide (N<sub>2</sub>O) fluxes, and carbon dioxide (CO<sub>2</sub>) emissions (ecosystem respiration) across coastal wetlands were estimated as  $2.20 \pm 0.31 \text{ mg} \cdot \text{m}^{-2} \cdot \text{h}^{-1}$ ,  $16.44 \pm 2.96 \text{ } \mu\text{g} \cdot \text{m}^{-2} \cdot \text{h}^{-1}$ , and  $388.76 \pm 42.28 \text{ mg} \cdot \text{m}^{-2} \cdot \text{h}^{-1}$ , respectively. GHG fluxes varied with tidal inundation, where CH<sub>4</sub> and CO<sub>2</sub> emissions during tidal inundation were lower than ebbing. CH<sub>4</sub> and CO<sub>2</sub> emissions from wetlands decreased linearly with increasing latitude; N<sub>2</sub>O did not. CH<sub>4</sub> fluxes were positively related to air temperature and aboveground biomass, and CO<sub>2</sub> emissions were positively related to soil organic carbon. N<sub>2</sub>O fluxes were lower with increasing soil pH, and CH<sub>4</sub> and CO<sub>2</sub> emissions were greater with increasing soil moisture. Based on the results of sustained-flux global warming potential and sustained-flux global cooling potential models, our paper indicated that the fluxes of CH<sub>4</sub> and N<sub>2</sub>O in coastal wetlands have a positive feedback to global warming, which is mainly driven by the CH<sub>4</sub> emission. Our synthesis improved understanding of the roles of coastal wetlands in the ecosystem C cycle under global change. We suggest that long-term field observations of GHG fluxes across a wider range of spatiotemporal scales are urgently required to improve the prediction accuracy in GHG fluxes and the assessment of net GHG balance and its contribution to the GWP of coastal wetlands.

**Keywords:** Coastal wetland; Plant invasion; Carbon cycle; Global warming; China

## **Hightlights**

- A first review was conducted on GHGs fluxes in the coastal wetlands of China.
- CH<sub>4</sub> and CO<sub>2</sub> emissions decreased linearly with increasing latitude, while N<sub>2</sub>O did not.
- Warming and plant invasion increase the risk of GHG emissions from coastal wetlands.
- Long-term observations are required to improve the prediction accuracy in GHG fluxes.

## 1. Introduction

A recent IPCC special report suggested that, at the current rate of increase, global warming is likely to reach 1.5°C between 2030 and 2052 and will significantly increase climate-related risks for natural and human systems (IPCC, 2018). More than 90% of global climate warming is attributable to increasing atmospheric concentrations of greenhouse gases (GHGs) derived from natural and anthropogenic sources (He et al., 2016; IPCC, 2013). Globally, carbon dioxide (CO<sub>2</sub>) is the most abundant greenhouse gas in the atmosphere and represents approximately 76% of total GHG emissions (IPCC, 2014); methane (CH<sub>4</sub>) and nitrous oxide (N<sub>2</sub>O) also contribute to global warming, with respective relative global warming potentials 28 and 265 times greater than that of CO<sub>2</sub> at a 100-year horizon (IPCC, 2014). GHG emissions from various ecosystems have thus become one of the key issues in ecology and global change research (O'Connell et al., 2018; Yu et al., 2013). Although wetlands occupy only 6% of the earth's land surface (Flury et al., 2010), they play an important role in carbon (C) sequestration and have been identified as important GHG sources and sinks (Olefeldt et al., 2017). GHG emissions from wetland ecosystems show high levels of spatiotemporal variability, depending on wetland type (Olefeldt et al., 2017; Turetsky et al., 2014), soil properties (Estop-Aragonés et al., 2016), and climatic conditions (Nahlik and Mitsch, 2011). Of the factors, wetland type is an important factor affecting GHG emissions; therefore, it may be used to provide credible estimates of global GHG fluxes from wetland ecosystems (Turetsky et al., 2014).

Coastal wetlands are globally distributed and are among the most productive ecosystems that play an important role in C sequestration and nutrient cycling (Collins et al., 2017; Kirwan and Megonigal, 2013). GHG fluxes from coastal wetlands have been intensively studied, and their functions as sinks (negative values, uptake) and sources (positive values, emissions) for atmospheric GHG emissions have been reported. For example, Chmura (2013) confirmed that coastal wetlands sequester significant amounts of CO<sub>2</sub>, whereas

Wilson et al. (2015) found that coastal wetlands were a net C source to the atmosphere as a result of high levels of ecosystem respiration. Most researchers believe that there is a significant negative correlation between methanogenesis and salinity, which really depends on the availability of sulfate (Eriksson et al., 2010; Gauci et al., 2015; Purdy et al., 2003). But, a meta-analysis by Poffenbarger et al. (2011) found that there was no significant difference in CH<sub>4</sub> emissions between freshwater and mesohaline marshes (4.8±8.7 and 1.8±1.3 mg·m<sup>-2</sup>·h<sup>-1</sup>, respectively), while oligohaline (0.5-5) marshes had the highest CH<sub>4</sub> emissions (17.1±25.2 mg·m<sup>-2</sup>·h<sup>-1</sup>). Similarly, there are contrasting reports of N<sub>2</sub>O fluxes from coastal wetlands; for example, Xu et al. (2014) found that coastal wetlands are dominant sources of N<sub>2</sub>O emissions (from 1.5 to 65.7 mg·m<sup>-2</sup>·h<sup>-1</sup>), whereas Daniel et al. (2013) reported that estuarine wetlands have an inverse source-sink function for N<sub>2</sub>O fluxes (from -108.2 to 51.3 mg·m<sup>-2</sup>·h<sup>-1</sup>) that may be attributed to ecosystem balances in hydrology and nutrients. These apparently conflicting findings indicate that source-sink dynamics of GHGs may vary across coastal wetland ecosystems due to site-specific environmental conditions (Falkowski et al., 2000); however, few studies have explicitly linked site-specific environmental factors with GHG fluxes from coastal wetlands, which limits our understanding of the mechanistic processes involved in GHG emissions (Zhu et al., 2013). Therefore, quantification of magnitudes and patterns of coastal wetland GHG fluxes at regional and/or global scales is critical to understanding global climate change processes and to the accurate prediction of future climate change trends (Falkowski et al., 2000; Yu et al., 2013).

The coastline of China extends for approximately  $1.8 \times 10^4$  km and comprises a coastal wetland area of approximately  $579.59 \times 10^4$  ha, which represents 12.42% of the total area of natural wetlands in China (Sun et al., 2015). However, the area of coastal wetlands in China has sharply decreased with rapid economic development and frequent human interference (Hu et al., 2018), which endangers C sequestration and other ecosystem services (Davidson et al., 2018). Although previous work has revealed total patterns and fluxes of GHG in different Chinese wetlands, data from coastal wetlands are lacking (Chen et al., 2013; Yu et al., 2013).

For example, Chen et al. (2013) summarized results for CH<sub>4</sub> emissions from rice paddies, natural wetlands, and lakes in China and found that rice paddies in southeastern China were the greatest source of CH<sub>4</sub>, accounting for approximately 55% of total emissions. Lu et al. (2016) compared ecosystem CO<sub>2</sub> fluxes among inland and coastal wetlands across the globe based on eddy covariance data and suggested that coastal wetlands provided larger CO<sub>2</sub> sinks than inland wetlands on a per unit area basis. A recent synthesis estimated C uptake and emissions of wetland ecosystems in China and suggested that C stocks, uptakes and gaseous losses varied with wetland type, whereas the method chosen in their analysis only included the eddy covariance technique (Xiao et al., 2019). Previous studies were primarily conducted in inland wetland or constructed wetland (rice paddy), and mostly examined CO<sub>2</sub>, CH<sub>4</sub> and N<sub>2</sub>O separately, and a comprehensive understanding of the magnitude and patterns of the three major GHG fluxes is not available for coastal wetlands in China.

In this study we conducted a comprehensive analysis of published data of the fluxes of the three major GHGs in the coastal wetlands of China to quantify their magnitude and identify the key drivers of the fluxes. Our objective was to answer the following questions: (1) what are the magnitudes and patterns of GHG fluxes across coastal wetlands in China, (2) what are the critical drivers that control GHG fluxes in coastal wetlands, and (3) what is the contribution of coastal wetland GHG fluxes in China to the Global Warming Potential?

## **2. Materials and methods**

### ***2.1. Literature search and data criteria***

We conducted a systematic analysis of peer-reviewed literature on GHG fluxes from coastal wetlands in China, from which we extracted data for individual field measurements of fluxes in at least one of the measured GHGs. The dataset was maximized by searching for papers published in English or Chinese before 31 December 2018 using the Web of Science (<http://apps.webofknowledge.com/>) and the China Knowledge Resource Integrated Database (<http://www.cnki.net/>). Publications were searched using the terms: China AND

(coastal wetland OR salt marsh OR tidal wetland OR brackish marsh OR estuarine marsh) in combination with the terms (CH<sub>4</sub> OR CO<sub>2</sub> OR N<sub>2</sub>O OR methane OR carbon dioxide OR ecosystem respiration OR nitrous oxide OR greenhouse gas OR carbon flux); this search yielded 203 publications. Then, publication bias was minimized using the following criteria: (1) GHG fluxes were measured from natural coastal wetlands in China under field conditions using a replicated experimental design; (2) field studies used the static chamber-gas chromatography method; and (3) only single plant communities were included. Following application of these criteria, we selected a total of 70 peer-reviewed publications involving 187 observations from 7 coastal provinces or Special Administrative Regions. Although some observations had data available for all the GHG fluxes (CH<sub>4</sub>, CO<sub>2</sub>, and N<sub>2</sub>O), some observations only had one or two GHG fluxes. Therefore, the number of observations varied with the type of GHG flux, which consisted of 132, 68, and 60 observations for CH<sub>4</sub>, CO<sub>2</sub>, and N<sub>2</sub>O fluxes, respectively. Most of the selected observations after 2007, with the earliest published in 1995, may reflect the trend in recent increases in quantitative studies of GHG fluxes from coastal wetlands in China (Appendix S1). The geographic distribution of the selected studies along the Chinese coast is presented in [Fig. 1](#).

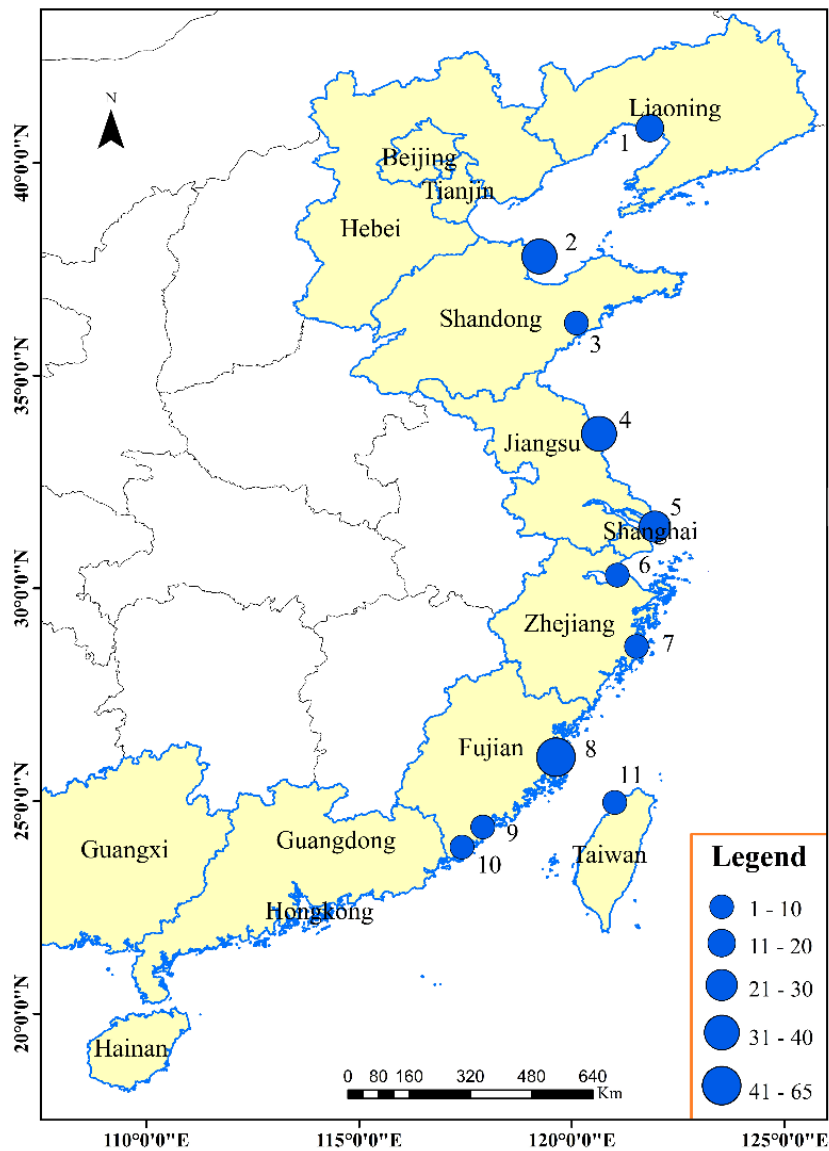


**Fig. 1.** Distribution and numbers of observations of the coastal wetlands along the coast of China included in this synthesis. Bubble size represents the number of observations in the same regions. The numbers on the figure represents: 1. Liaohe estuary; 2. Yellow River estuary; 3. Jiaozhou Bay; 4. Yancheng coastal wetland; 5. Yangtze River estuary; 6. Hangzhou Bay; 7. Taizhou coastal wetland; 8. Min River estuary; 9. Jiulong River estuary; 10. Zhangjiang River estuary; and 11. Kuan-du wetland.

## 2.2. Data extraction and aggregation

Raw data were extracted from the selected publications, either directly from tables and texts or from figures, using GetData Graph Digitizer software (version 2.22, <http://www.getdatagraph-digitizer.com/>).

Several publications did not provide direct data on GHG fluxes but related data that could be used for

estimation. Specifically, CO<sub>2</sub> equivalent (CO<sub>2</sub>-eq ha<sup>-1</sup>) data were divided by 296 for N<sub>2</sub>O and by 23 for CH<sub>4</sub>, respectively (IPCC, 2007; Zhao et al., 2016). Daily or seasonal cumulative GHG fluxes were calculated by dividing flux data by the corresponding observation time, and data for fluxes reported as molar CH<sub>4</sub>, CO<sub>2</sub> and N<sub>2</sub>O were transformed using molecular mass as a conversion factor. Data derived from multiple growing seasons and/or years were used to calculate mean fluxes over a single observation, and only data from untreated control plots were used where a study was composed of experimental treatments. Moreover, if a paper reported data from multiple study sites, each site was included as independent observations. In coastal wetlands, CO<sub>2</sub> emission represent ecosystem-derived CO<sub>2</sub> (ecosystem respiration) due to the measurement of CO<sub>2</sub> emissions using the enclosed static opaque chamber-GC technique, in which plants are included. Data were provided as raw values of instantaneous GHG fluxes and then subsequently converted to standardized units of mg·m<sup>-2</sup>·h<sup>-1</sup> for CH<sub>4</sub> and CO<sub>2</sub> and of μg·m<sup>-2</sup>·h<sup>-1</sup> for N<sub>2</sub>O.

Ancillary study site variables included location (longitude and latitude) and climate type, dominant species, mean annual temperature, study duration and season, frequency of measurements and number of replicates, soil properties (including soil pH and organic C (SOC) at 0-20 cm depth), and porewater salinity and SO<sub>4</sub><sup>2-</sup> concentrations. When only soil organic matter data were available, they were converted to SOC using a conversion factor of 1.724 for the surface horizons to maximize data use (Nelson and Sommers, 1996). If data were unavailable for a given study, we cross-referenced studies from the same location to search for the missing information. Data used in this synthesis are listed in Appendix S1.

To better understand the factors that regulate the magnitudes and patterns of GHG fluxes in coastal wetlands, auxiliary variables were grouped to facilitate cross-comparison between studies, including vegetation type (single dominant plant communities and nonvegetated mudflats), climate zone (temperate and subtropical), tidal flats (high, middle, and low marsh), and tidal process (before flooding, flooding and ebbing process, and after ebbing). GHG fluxes in different tidal flats were extracted directly from the published studies,

which were classed based on the relative position of the mean high water (Bertness, 1991). Moreover, we defined mudflats as muddy or sandy flats behind vegetated wetlands. The total area of coastal wetlands in China was estimated to be approximately 2320.5 km<sup>2</sup> (Niu et al., 2012; Zhou et al., 2016; Zuo et al., 2012).

### 2.3. Estimation of global warming potential

Neubauer and Megonigal (2015) presented an improved method of GWP evaluation based on sustained-flux global warming potential (SGWP) for gas emissions and sustained-flux global cooling potential (SGCP) for gas uptake models. In this synthesis, we quantified and compared the radiative forcing of the fluxes of CH<sub>4</sub> and N<sub>2</sub>O in coastal wetlands, based on SGWP and SGCP over a 100-year horizon, using the following equation (Neubauer and Megonigal, 2015):

$$F = SGWP \times EF_{CH_4} + SGWP \times EF_{N_2O} - SGCP \times INF_{CH_4} - SGCP \times INF_{N_2O} \quad (1)$$

where  $F$  is the CO<sub>2</sub>-equivalent flux (kg CO<sub>2</sub>eq ha<sup>-1</sup>);  $SGWP$  and  $SGCP$  are the sustained-flux global warming and sustained-flux global cooling potentials of CH<sub>4</sub> and N<sub>2</sub>O on a 100-year horizon (respective potential values are 45 and 270) (Neubauer and Megonigal, 2019);  $EF_{CH_4}$  and  $EF_{N_2O}$  are average CH<sub>4</sub>, and N<sub>2</sub>O effluxes (mg·m<sup>-2</sup>·h<sup>-1</sup>), respectively; and,  $INF_{CH_4}$  and  $INF_{N_2O}$  are average CH<sub>4</sub> and N<sub>2</sub>O influxes (mg·m<sup>-2</sup>·h<sup>-1</sup>), respectively.

### 2.4. Statistical analysis

Given the large differences in spatial distribution and sample size among the different gas types and categorical groups, normal distribution and homogenous variance of the data were first tested. A three-factor repeated-measures multivariate analysis of variance (MANOVA) was employed to evaluate the effects of dominant species (*S. alterniflora* vs *P. australis*), season, climate zone (temperate vs subtropical), and their interactions on GHG fluxes using R version 3.5.1 (R Development Core Team, 2020). Pearson correlation

analyses were performed to determine relationships between GHG fluxes and environmental variables. Statistical significance was set at  $P < 0.05$ .

We employed a linear mixed-effect model (LMM) to examine the relationships between GHG ( $\text{CO}_2$ ,  $\text{CH}_4$ , and  $\text{N}_2\text{O}$ ) fluxes and environmental variables, and attempts were made to obtain the best model for explaining the maximum variability of the GHG fluxes. Briefly, for each variable ( $X$ ), we tested the relationship between GHG and  $X$  using the model (Li et al., 2019; Tian et al., 2018):

$$\ln(\text{GHG}) = \beta_0 + \beta_1 \times X + \pi_{\text{study}} + \varepsilon \quad (2)$$

where  $\beta_0$ ,  $\beta_1$ ,  $\pi_{\text{study}}$ , and  $\varepsilon$  are the intercept, coefficient, random effect, and sampling error, respectively. The random effect accounts for autocorrelation among observations within each “study site”. We conducted the analyses using the maximum likelihood estimation with the *lme4* and *lmerTest* packages (Bates et al., 2018). The slopes between GHG and variables (climate, soil, and plant properties) were extracted and plotted into a scatter figure with 95% confidence intervals.

Moreover, structural equation models (SEM) was applied to investigate the direct and indirect effects of climate, soil and vegetation factors to the observed variations in GHG fluxes. Specifically, we standardized environmental factors in the best model of GHG fluxes at first, and then took it as observed variables to evaluate the direct and indirect effects of environmental factors and their interactions on each GHG fluxes using SEM models, based on the maximum likelihood estimation method (Oberski, 2014). The SEM analyses were performed with the *lavaan* package using R version 3.6.3 software (R Development Core Team, 2020).

### **3. Results**

#### ***3.1. GHG fluxes across coastal wetlands***

Overall, the magnitudes and trends of GHG fluxes across coastal wetlands varied with species, hydrology

and wetlands types (Fig. 2). CH<sub>4</sub>, N<sub>2</sub>O fluxes, and CO<sub>2</sub> emissions ranged from -0.14 to 15.90 mg·m<sup>-2</sup>·h<sup>-1</sup>, -17.82 to 109.72 μg·m<sup>-2</sup>·h<sup>-1</sup>, and -13.56 to 1456.6 mg·m<sup>-2</sup>·h<sup>-1</sup>, respectively, with respective averages of 2.20±0.31 mg·m<sup>-2</sup>·h<sup>-1</sup>, 16.44±2.96 μg·m<sup>-2</sup>·h<sup>-1</sup>, and 388.76±42.28 mg·m<sup>-2</sup>·h<sup>-1</sup>. Coefficients of variation (CVs) for CH<sub>4</sub>, N<sub>2</sub>O, and CO<sub>2</sub> were 161.90, 139.29, and 89.68 %, respectively. GHG fluxes differed within the biotic and abiotic groups of variables. Among vegetation types, average CH<sub>4</sub> fluxes were greatest (7.88±1.01 mg·m<sup>-2</sup>·h<sup>-1</sup>) in *Sagittaria trifolia*-dominated wetlands and lowest (-0.02±0.01 mg·m<sup>-2</sup>·h<sup>-1</sup>) in wetlands dominated by *Artemisia schrenkiana* (only one observation). Average CO<sub>2</sub> emissions were greatest (720.77 ±121.32 mg·m<sup>-2</sup>·h<sup>-1</sup>) in *Cyperus malaccensis*-dominated wetlands and lowest (77.64 ±63.34 mg·m<sup>-2</sup>·h<sup>-1</sup>) in wetlands dominated by *Tamarix chinensis*, and N<sub>2</sub>O fluxes were greatest (58.06 ±23.07 μg·m<sup>-2</sup>·h<sup>-1</sup>) in *S. trifolia* wetlands and lowest (4.32±3.74 μg·m<sup>-2</sup>·h<sup>-1</sup>) in *Phragmites australis* wetlands. CH<sub>4</sub> emissions and CO<sub>2</sub> fluxes were greater in *Spartina alterniflora*-dominated wetlands relative to most native species, whereas N<sub>2</sub>O fluxes did not differ. Nonvegetated mudflats efficiently reduced GHG fluxes compared with plant-dominated wetlands, and GHG fluxes varied with tidal processes, where average CH<sub>4</sub> and CO<sub>2</sub> emissions during tidal inundation were lower than during ebbing. There were some variations in GHG fluxes among coastal wetland types, where CH<sub>4</sub> and N<sub>2</sub>O fluxes in estuarine wetlands were greater than in coastal tidal-flats, but there were no differences in CO<sub>2</sub> emissions. Moreover, pooled climate-zone data showed that average GHG fluxes were greater in subtropical regions than in temperate regions.

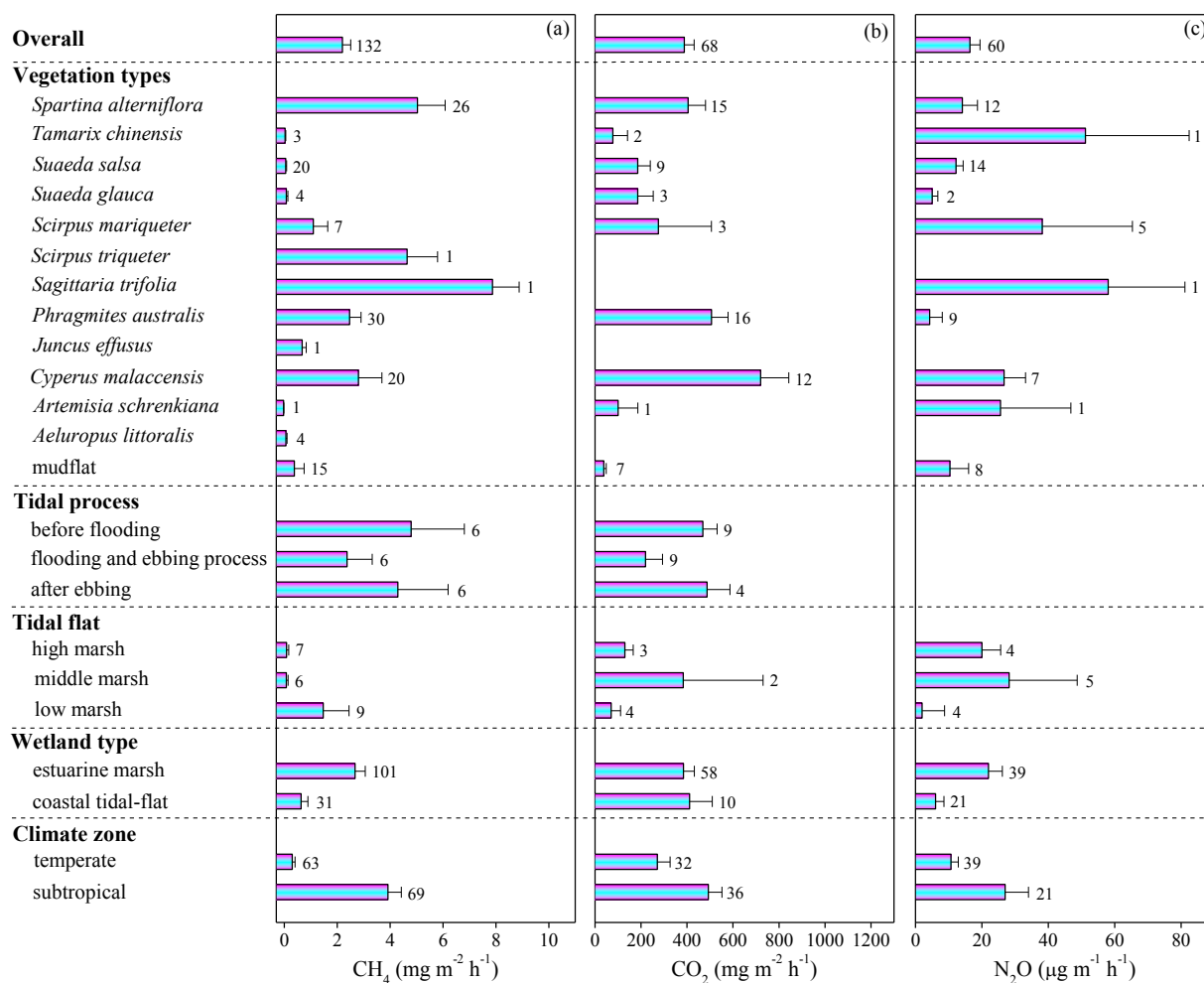


**Fig. 2.** Abiotic and biotic within-group differences in mean CH<sub>4</sub>, CO<sub>2</sub>, and N<sub>2</sub>O fluxes from the coastal wetlands. Data represent the mean ( $\pm$ SE), which was calculated by integrating all observations within each group. Numbers next to the error bars are numbers (*n*) of observations for each variable. “Overall” represents the overall mean ( $\pm$ SE) GHG fluxes extracted from all observations; some grouped data were only extracted from several observations, and the data volume in some groups were thus lower than the overall. Tidal flats were classed based on the relative position of the mean high water.

Spatially, mean CH<sub>4</sub> and CO<sub>2</sub> emissions from coastal wetlands decreased linearly with increasing latitude (Figs. 3a-b;  $P < 0.01$ ) but there was no effect of latitude on N<sub>2</sub>O fluxes (Fig. 3c). GHG fluxes showed a large spatial variation among study sites (Fig. S1), where coastal wetlands located in the Min River Estuary were the greatest source of CH<sub>4</sub> emissions (average: 47.22 g·m<sup>-2</sup>·y<sup>-1</sup>) and those in the Yellow River Estuary were the lowest (average: 0.33 g·m<sup>-2</sup>·y<sup>-1</sup>). CO<sub>2</sub> emissions were greatest in the Min River Estuary (average: 5130.05 g·m<sup>-2</sup>·y<sup>-1</sup>) and lowest in the Zhangjiang River Estuary (average: 50.28 g·m<sup>-2</sup>·y<sup>-1</sup>). Wetlands in the Jiulong

River Estuary represented the greatest source of N<sub>2</sub>O emissions (average: 0.34 g·m<sup>-2</sup>·y<sup>-1</sup>) and those at Yancheng were the smallest (average: 0.05 g·m<sup>-2</sup>·y<sup>-1</sup>). When summarizing all field measurements, annual mean CO<sub>2</sub>, CH<sub>4</sub>, and N<sub>2</sub>O fluxes from the coastal wetlands of China were roughly estimated to be 7902.58 Gg, 44.67 Gg, and 0.33 Gg, respectively.

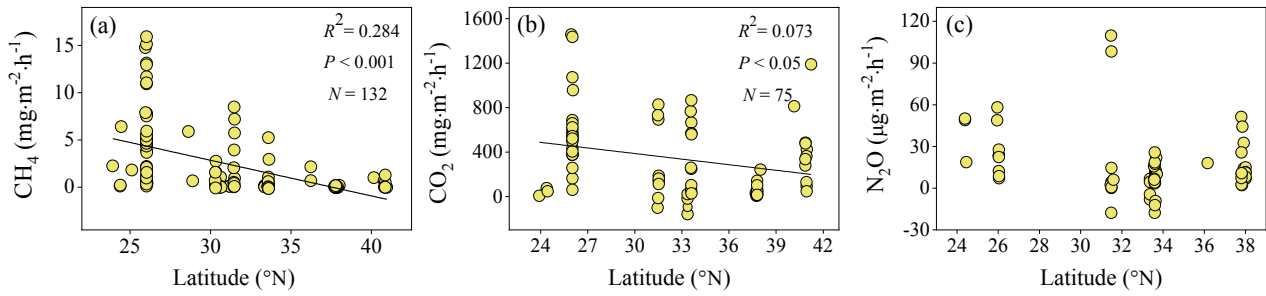


**Fig. 3.** Association between latitude and CH<sub>4</sub> (a), CO<sub>2</sub> (b), and N<sub>2</sub>O (c) fluxes in the coastal wetlands.

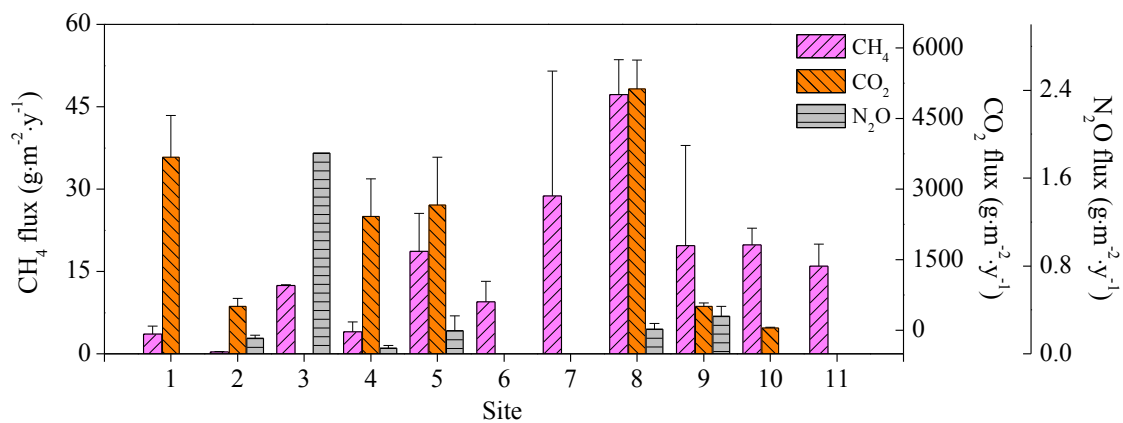


**Fig. S1** Annual GHG fluxes in different wetland sites included in this study. The numbers on the figure represent: 1. Liaohe estuary; 2. Yellow River estuary; 3. Jiaozhou Bay; 4. Yancheng coastal wetland; 5. Yangtze River estuary; 6. Hangzhou Bay; 7. Taizhou coastal wetland; 8. Min River estuary; 9. Jiulong River estuary; 10. Zhangjiang River estuary; and 11. Kuan-du wetland. The absence of boxes indicates an absence of flux data.

### 3.2. Environmental drivers of GHG fluxes across coastal wetlands

We analyzed the effects of climate, soil, and plant variables on GHG fluxes in the coastal wetlands (Figs. S2-S4). Specifically, CH<sub>4</sub> fluxes significantly increased with increasing air temperature ( $P < 0.01$ ; Fig. S2a), aboveground biomass ( $P < 0.001$ ; Fig. S2b), SOC ( $P < 0.05$ ; Fig. S2d), and soil moisture ( $P < 0.001$ ; Fig. S2e).

Similarly, soil pH and SOC were the main drivers of CO<sub>2</sub> emissions: CO<sub>2</sub> emissions were negatively related to soil pH ( $P < 0.05$ ; Fig. S3a), but positively related to SOC ( $P < 0.05$ ; Fig. S3b). Moreover, there were negative significant relationships between N<sub>2</sub>O fluxes and soil pH in the coastal wetlands ( $P < 0.01$ ; Fig. S4a).

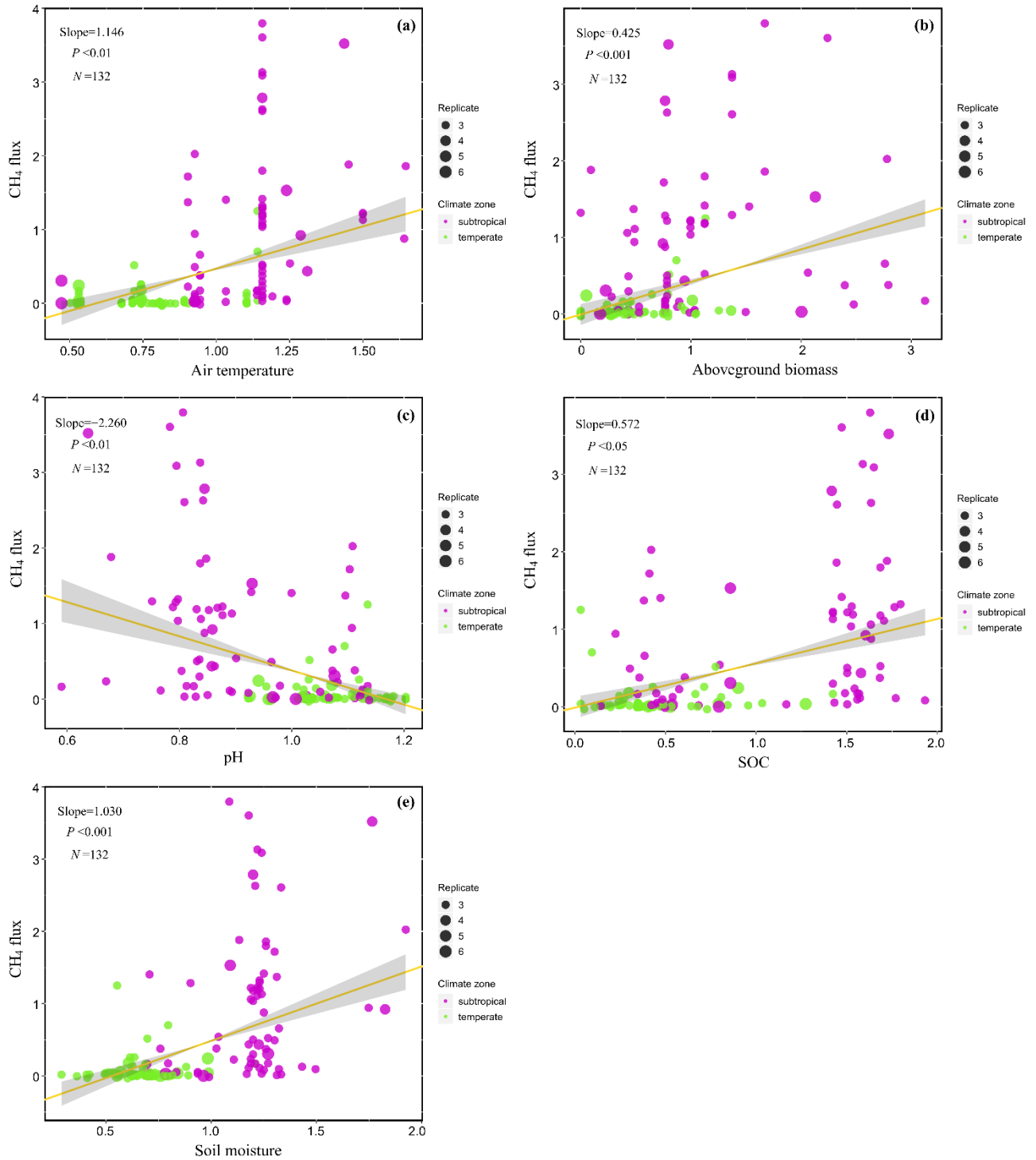


**Fig. S2** Bivariate relationships of CH<sub>4</sub> fluxes with air temperature (a), aboveground biomass (b), pH (c), SOC (d), and soil moisture (e) in the coastal wetlands of China. The values of air temperature, aboveground biomass, pH, SOC, and

soil moisture ranged from 8.0 to 27.9 (mean:  $16.4 \pm 4.2$ ),  $68.4$  to  $4237.0$  ( $1171.6 \pm 832.4$ )  $\text{g} \cdot \text{m}^{-2}$ ,  $4.6$  to  $9.4$  ( $7.7 \pm 1.1$ ),  $0.4$  to  $25.3$  ( $10.7 \pm 7.5$ )  $\text{g} \cdot \text{kg}^{-1}$ , and  $14.1$  to  $93.9$  ( $45.9 \pm 16.0$ ) %, respectively. The data were standardized (z-score normalization) to compare the responses of  $\text{CH}_4$  fluxes to environmental variables. For clarity, only significant variables were included in the figure ( $P < 0.05$ ). Yellow lines and thicker shaded areas represent the mean and 95% confidence intervals of the slope regressed by the linear mixed-effect model, respectively. The sizes of the bubbles represent the number of replicates of corresponding observations.  $N$  refers to the number of observations. The significance ( $P$ ) is presented for each term tested. SOC: soil organic carbon.

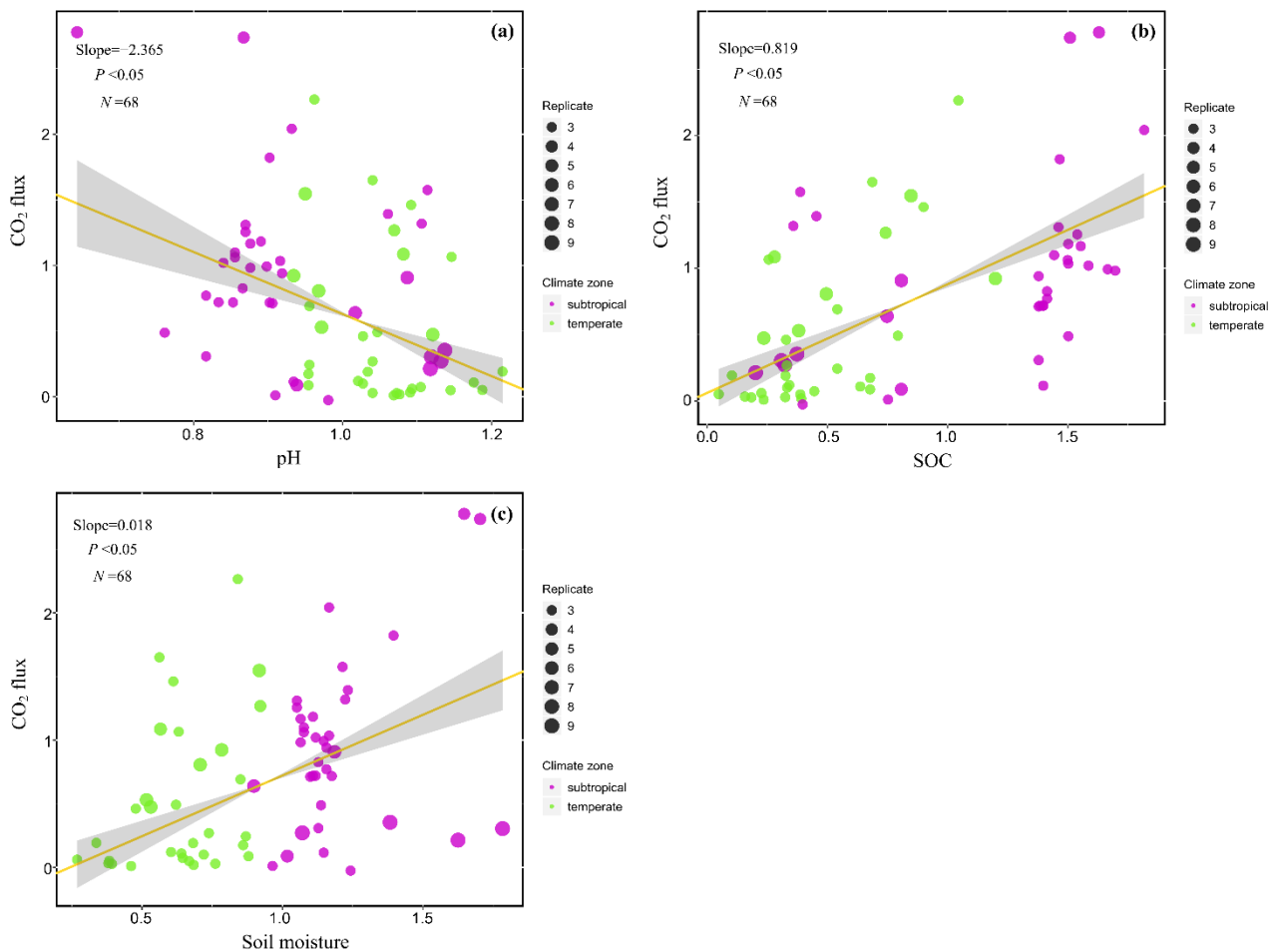


**Fig. S3** Bivariate relationships of  $\text{CO}_2$  emissions with selected soil pH (a), SOC (b), and moisture (c) in the coastal wetlands of China. For clarity, only significant variables were included in the figure ( $P < 0.05$ ). The values of pH, SOC, and soil moisture ranged from  $5.0$  to  $9.4$  (mean:  $7.6 \pm 0.9$ ),  $0.7$  to  $25.3$  ( $11.7 \pm 7.5$ )  $\text{g} \cdot \text{kg}^{-1}$ , and  $14.1$  to  $93.3$  ( $48.9 \pm 17.6$ ) %, respectively. The data were standardized (z-score normalization) to compare the responses of  $\text{CO}_2$  emissions to environmental variables. The yellow lines and thicker shaded areas represent the mean and 95% confidence intervals of the slope regressed by the linear mixed-effect model, respectively. The sizes of the bubbles represent the number of replicates of corresponding observations.  $N$  refers to the number of observations. The significance ( $P$ ) is presented for

each term tested. SOC: soil organic carbon.

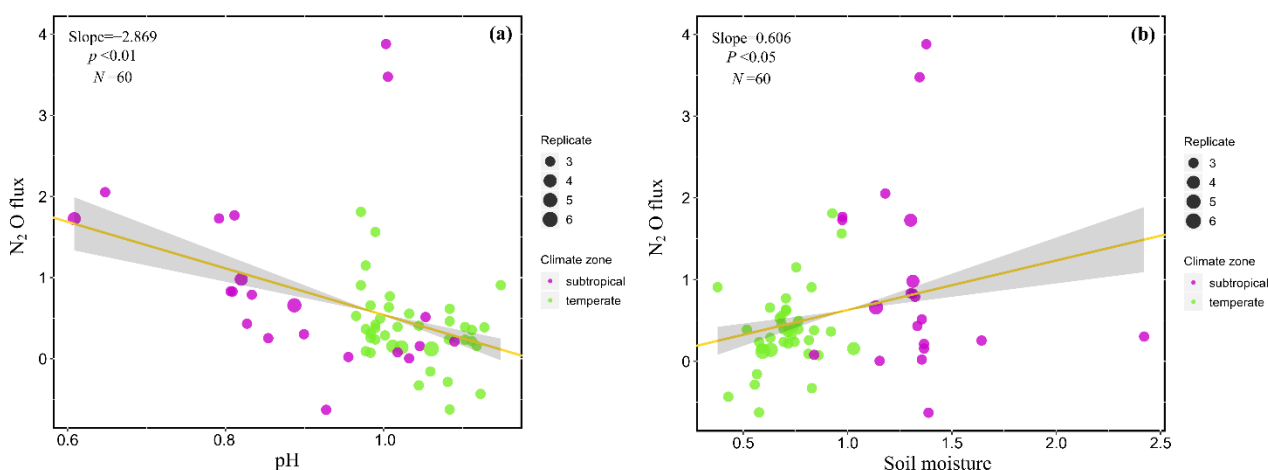


**Fig. S4** Bivariate relationships of  $N_2O$  fluxes with selected soil pH (a) and soil moisture (b) in the coastal wetlands of China. For clarity, only significant variables were included in the figure ( $P < 0.05$ ). The values of pH and soil moisture ranged from 5.0 to 9.4 (mean:  $8.1 \pm 0.9$ ) and 17.7 to 113.4 ( $43.3 \pm 16.9$  %), respectively. The data were standardized (z-score normalization) to compare the responses of  $N_2O$  fluxes to environmental variables. Yellow lines and thicker shaded areas represent the mean and 95% confidence intervals of the slope regressed by the linear mixed-effect model, respectively. The sizes of the bubbles represent the number of replicates of corresponding observations.  $N$  refers to the number of observations. The significance ( $P$ ) is presented for each term tested.

Our SEM results further indicated that the magnitudes and patterns of GHG fluxes from the coastal wetlands were driven by the synergistic effects of site-specific environmental factors (Fig. 4). Overall, the fixed factors in the model could explain 43.8, 40.0, and 16.3 % of the total variances, and further combinations from the fixed and random effects explained 43.8, 43.1, and 16.3% of the variance in  $CH_4$ ,  $CO_2$ , and  $N_2O$  fluxes, respectively. Specifically,  $CH_4$  fluxes were directly mediated by air temperature (path coefficient= 0.19) and aboveground biomass (path coefficient= 0.21). Moreover, air temperature also indirectly influenced  $CH_4$  fluxes by its effect on soil moisture (path coefficient = 0.50) and aboveground biomass (path coefficient = 0.28).  $CO_2$  emissions were directly affected by the SOC (path coefficient = 0.60) and indirectly upregulated by soil pH via its effect on SOC (path coefficient = 0.76).

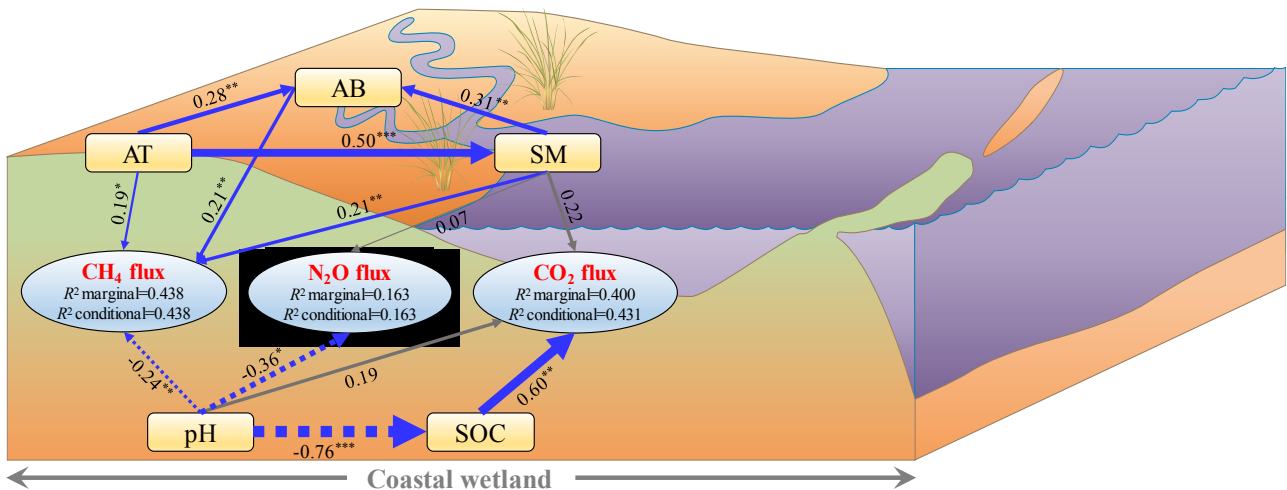


**Fig. 4.** Structural equation model (SEM) showing the direct and indirect effects of environmental parameters (climate, soil and plant-related parameters) to GHG fluxes in the coastal wetlands. The number of samples finally included in the SEM models were 132, 68, and 60 for CH<sub>4</sub>, CO<sub>2</sub>, and N<sub>2</sub>O, respectively. Blue solid and dotted lines represent positive and negative relationships, respectively. Gray lines refer to nonsignificant relationships. Line width indicates the strength of the relationship. The numbers alongside the lines are standardized path coefficients.  $R^2$  marginal and  $R^2$  conditional refer to the degree of variation of the variable explained by all paths from the single fixed effects and both the fixed and random effects (study site), respectively. Significance levels are as follows: \* $P < 0.05$ , \*\* $P < 0.01$ , and \*\*\* $P < 0.001$ . AT: Air temperature; SM: soil moisture; SOC: soil organic carbon; AB: aboveground biomass.

### 3.3. Estimated GWP from coastal wetlands

To assess the climate role of emissions of CH<sub>4</sub> and N<sub>2</sub>O from coastal wetlands, we estimated the CO<sub>2</sub>-equivalent of CH<sub>4</sub> and N<sub>2</sub>O emissions over a 100-yr time horizon based on calculations of SGWP (emissions) and SGCP (uptake). The results showed that the CO<sub>2</sub>-equivalent of the coastal wetlands was about 10.40 Mg·CO<sub>2</sub>eq·ha<sup>-1</sup>·y<sup>-1</sup> (Table 1), in which, SGWP was approximately 30 times greater than SGCP. Our findings initially indicated that coastal wetlands have a positive feedback to global warming, without considering C sequestration of tidal marsh ecosystem. Further, for coastal wetlands, this positive feedback is driven by the emission of CH<sub>4</sub>, which (in equivalents of kg CO<sub>2</sub> m<sup>-2</sup>·y<sup>-1</sup>) is sufficient to offset the effect of uptake of N<sub>2</sub>O (Table 1).

**Table 1** Annual average fluxes and CO<sub>2</sub> equivalents of CH<sub>4</sub> and N<sub>2</sub>O emissions in coastal wetlands based on SGWP and

SGCP over a 100-year time horizon.

Annual fluxes ( $\text{g}\cdot\text{m}^{-2}\cdot\text{y}^{-1}$ )		CO <sub>2</sub> equivalent t ( $\text{Mg}\cdot\text{ha}^{-1}\cdot\text{y}^{-1}$ )				Total CO <sub>2</sub> eq ( $\text{Mg}\cdot\text{ha}^{-1}$ )
CH <sub>4</sub>	N <sub>2</sub> O	SGWP for CH <sub>4</sub>	SGWP for N <sub>2</sub> O	SGCP for CH <sub>4</sub>	SGCP for N <sub>2</sub> O	
19.25	0.14	10.32	0.46	0.11	0.27	10.40

SGWP: sustained-flux global warming potential (for gas emissions); SGCP: sustained-flux global cooling potential (for gas uptake).

It is worth noting that CO<sub>2</sub> in this synthesis refers to ecosystem respiration and is therefore not included in this estimation. GWP was calculated using the difference between SGWP and SGCP. Mg = 10<sup>3</sup> kg.

## 4. Discussion

### 4.1. Magnitudes and spatial patterns of GHG fluxes across coastal wetlands

Due to high spatial heterogeneity within the coastal wetlands, we found that there was great variation in GHG fluxes, particularly of CH<sub>4</sub> (CV = 161.90%) and N<sub>2</sub>O (CV = 139.29%). Compared with other analyses of GHG fluxes from wetlands, we found that average CH<sub>4</sub> fluxes from these coastal wetlands ( $2.20\pm 0.31 \text{ mg}\cdot\text{m}^{-2}\cdot\text{h}^{-1}$ ) were lower than fluxes from rice paddies ( $11.35\pm 12.41 \text{ mg}\cdot\text{m}^{-2}\cdot\text{h}^{-1}$ ), freshwater wetlands ( $9.71\pm 5.53 \text{ mg}\cdot\text{m}^{-2}\cdot\text{h}^{-1}$ ), and peatlands ( $6.46\pm 6.60 \text{ mg}\cdot\text{m}^{-2}\cdot\text{h}^{-1}$ ) across China, as reported by Chen et al. (2013). However, CO<sub>2</sub> emissions ( $388.76\pm 42.28 \text{ mg}\cdot\text{m}^{-2}\cdot\text{h}^{-1}$ ) were greater than those reported by Lu et al. (2016) from a global dataset of 22 inland wetlands ( $39.17 \text{ mg}\cdot\text{m}^{-2}\cdot\text{h}^{-1}$ ; ecosystem respiration) and 21 coastal wetlands ( $87.64 \text{ mg}\cdot\text{m}^{-2}\cdot\text{h}^{-1}$ ). In addition, GHG fluxes from coastal wetlands in China are different from other countries or regions. For example, in North America, Bartlett et al. (1987) measured CH<sub>4</sub> fluxes at three salt marshes along a tidal creek, found that CH<sub>4</sub> flux was  $2.08\pm 0.66 \text{ mg}\cdot\text{m}^{-2}\cdot\text{h}^{-1}$  at the freshest site (2.6±0.55 ppt),  $2.56\pm 0.39 \text{ mg}\cdot\text{m}^{-2}\cdot\text{h}^{-1}$  at the mid-salinity site (5.5±0.55 ppt), and  $0.64\pm 0.08 \text{ mg}\cdot\text{m}^{-2}\cdot\text{h}^{-1}$  at the most saline site (8.8±0.36 ppt). Holm et al. (2016) observed that CH<sub>4</sub> fluxes were  $7.11 \text{ mg}\cdot\text{m}^{-2}\cdot\text{h}^{-1}$  and  $1.58 \text{ mg}\cdot\text{m}^{-2}\cdot\text{h}^{-1}$  for the freshwater and brackish (8-10 ppt) sites of the Mississippi River Delta, respectively. These are higher than our reports in China's coastal wetlands, suggesting that GHG fluxes from coastal wetlands are site-dependent and highly variable. Lower CH<sub>4</sub> fluxes from coastal wetlands are possibly due to higher salinity and SO<sub>4</sub><sup>2-</sup> concentrations, which trigger sulfate-reducing bacteria (SRB) to outcompete methanogens for energy sources due to the greater

affinity of SRB for acetate, H<sub>2</sub>, and other substrates, which leads to inhibited CH<sub>4</sub> production (Purdy et al., 2003). In this synthesis, we found a negative relationship between salinity and CH<sub>4</sub> flux (Fig. 5), and further oligohaline systems (0.5–5) had significantly higher CH<sub>4</sub> emissions and variability than the other salinity levels. This finding is consistent with previous review by Poffenbarger et al. (2011), who also observed that oligohaline (0.5–5) marshes had the highest and most variable CH<sub>4</sub> emissions relative to the fresh (0–0.5), mesohaline (5–18), and polyhaline tidal marshes (salinity>18). These findings further confirmed that CH<sub>4</sub> fluxes decreased with increasing salinity, but there may be a threshold at about 0.5–5 salinity, above or below which the CH<sub>4</sub> emissions remain low and relatively stable. The greater CO<sub>2</sub> emissions estimated in this synthesis may be explained by the high levels of plant productivity and litter input in coastal wetlands that often results in greater root respiration and mineralization of SOC (Liu et al., 2014). Moreover, high salinity and ionic strength (SO<sub>4</sub><sup>2-</sup> and Cl<sup>-</sup>) in coastal wetlands may theoretically induce microbial osmotic stress, which would lead to cell lysis and the divergence of the microbial community, and the addition of SO<sub>4</sub><sup>2-</sup> enhances its significance as an electron acceptor, with the ratio of sulfate reduction and CO<sub>2</sub> production being 1:2 (Chambers et al., 2013).

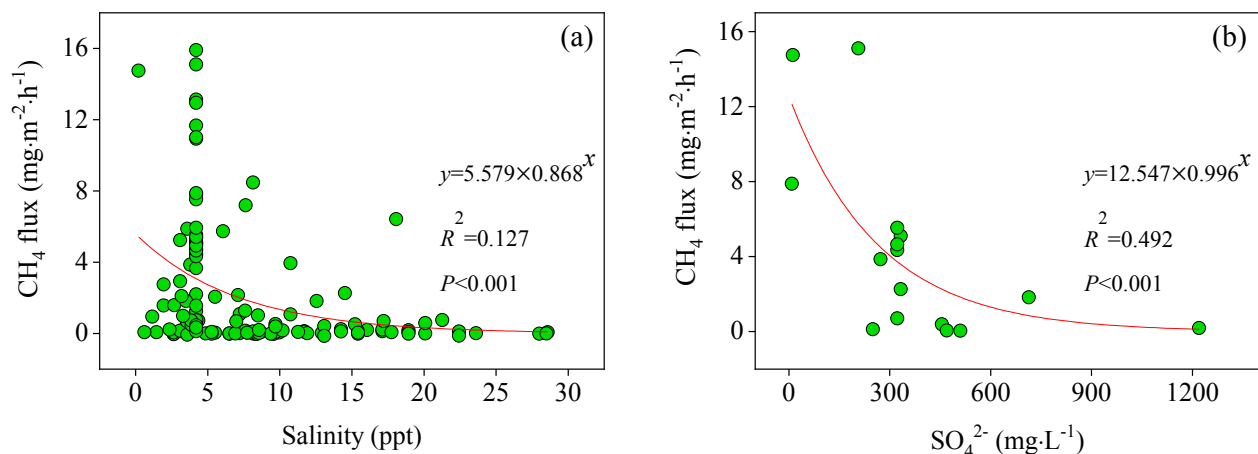


**Fig. 5.** Relationships between porewater salinity (a), SO<sub>4</sub><sup>2-</sup> (b) and GHG fluxes in the coastal wetlands.

Our analysis also showed that various abiotic and biotic factors, such as dominant species, tidal process, and wetland type, were drivers of variation in GHG fluxes (Fig. 2). For example, we found that CH<sub>4</sub> fluxes

were greater in the oligohaline marshes dominated by *S. alterniflora* (Fig. 2a). Similar patterns were observed by Tong et al. (2018) in an oligohaline marsh, who suggested that *S. alterniflora* supports higher rates of CH<sub>4</sub> production than native species via supplying more methane production substrates of acetate. *S. alterniflora* may also enhance CH<sub>4</sub> fluxes via improves in litter quality and the stimulation of methanogenesis by providing substrates for methanogens or aerenchyma (Qiu, 2015). GHG fluxes were found to be lower in nonvegetated mudflats than in vegetated wetlands (Fig. 2a), possibly because plant roots and stems act as a conduit for GHG release to the atmosphere (Laanbroek, 2010) and plant root exudates and other labile organic compounds released by plants stimulate the microbial community (Segarra et al., 2013). We found that flooded soil conditions, as found during tidal inundation (Fig. 2), inhibited GHG emissions. On the one hand, soil saturation or inundation causes anaerobic conditions and potentially hinders gas transport (Holm et al., 2016). On the other hand, we speculate that when flooded, the GHG produced by the soil will be released or diffused into the porewater or overlying water, reducing the flux to the atmosphere. Despite the wide range of species composition, hydrothermal conditions, and site history, CH<sub>4</sub> and CO<sub>2</sub> emissions decreased with increasing latitude for coastal wetlands (Fig. 3), especially for CH<sub>4</sub> fluxes (Fig. 3a), probably because latitude is a surrogate metric for temperature and precipitation (Lu et al., 2016; Yu et al., 2013).

#### **4.2. Differences in GHG fluxes for single dominant communities**

To reduce the multifactor interaction, we attempted to investigate the variation of GHG fluxes with latitude, season, and climate zone for two single communities, *S. alterniflora* (representative of invasive species) and *P. australis* (representative of native species), which are the two most widely distributed communities along the coast of China. Our data showed that mean CH<sub>4</sub> and N<sub>2</sub>O fluxes in *S. alterniflora*-dominated wetlands decreased linearly with increasing latitude (Figs. 6a, c;  $P < 0.001$  or  $P < 0.05$ ), whereas CO<sub>2</sub> fluxes showed the opposite trend (Fig. 6b;  $P < 0.05$ ). CH<sub>4</sub> fluxes in *P. australis*-dominated wetlands

decreased linearly with increasing latitude (Fig. 6d;  $P < 0.001$ ) but there was no effect of latitude on CO<sub>2</sub> emissions and N<sub>2</sub>O fluxes (Figs. 6e, f). MANOVA showed that variable species composition and climate zone had a significantly large effect on CH<sub>4</sub> and N<sub>2</sub>O fluxes and that seasonal changes significantly affected CH<sub>4</sub> fluxes and CO<sub>2</sub> emissions (Table 2). Moreover, the interaction of species and climate zones typically had a significant effect on CO<sub>2</sub> emissions and N<sub>2</sub>O fluxes across the coastal wetlands. These findings highlight the role of species and temperature as a primary environmental control on GHG fluxes, which indicates that future shifts in species composition- and warming-associated changes in soil nutrient dynamics may greatly affect GHG fluxes and exacerbate soil C loss in the coastal wetlands.

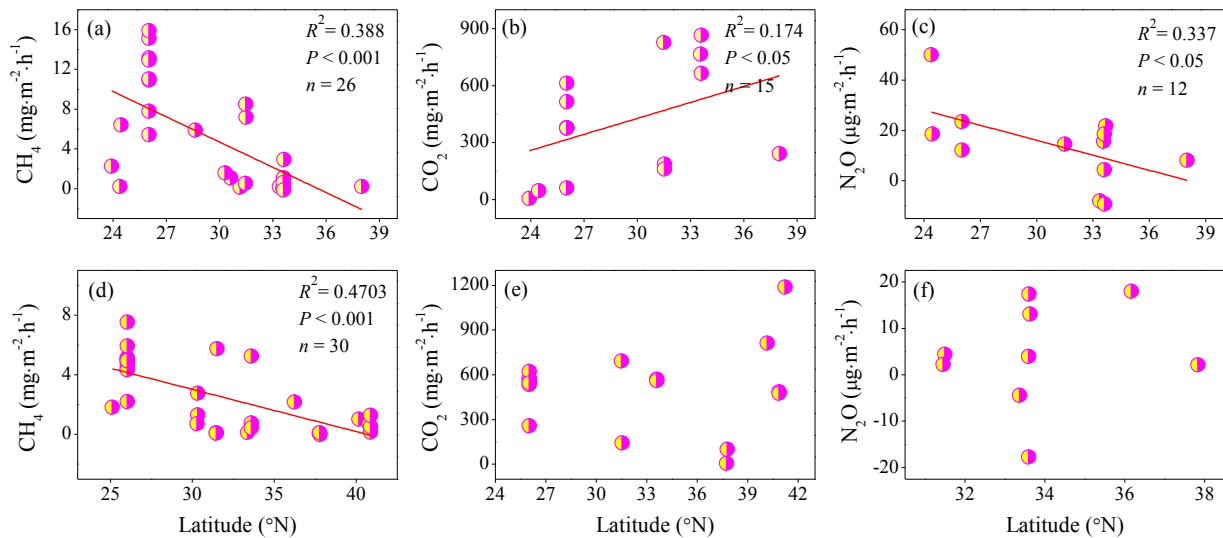


**Fig. 6.** Latitudinal patterns of GHG fluxes for single dominant plant communities of *Spartina alterniflora* (a, b, and c) and *Phragmites australis* (d, e, and f).

**Table 2** Results of repeated measures ANOVA indicating the effects of dominant species (*S. alterniflora* vs *P. australis*), season, climate zone (temperate vs subtropical), and their interactions on GHG fluxes.

Source of variation	CH <sub>4</sub> (mg·m <sup>-2</sup> ·h <sup>-1</sup> )		CO <sub>2</sub> (mg·m <sup>-2</sup> ·h <sup>-1</sup> )		N <sub>2</sub> O (μg·m <sup>-2</sup> ·h <sup>-1</sup> )	
	F	P	F	P	F	P
season	4.382	<0.01	12.957	<0.001	0.470	0.705
species	25.991	<0.001	0.777	0.380	3.999	<0.05
climate	11.828	<0.01	1.189	0.278	6.498	<0.05
species×season	1.176	0.320	0.036	0.991	0.472	0.704
season×climate	0.278	0.842	2.336	0.078	1.112	0.354
species×climate	0.744	0.390	7.976	<0.01	5.159	<0.05

Moreover, *S. alterniflora*, which began to be planted in the coastal wetlands of China in ecological restoration programs in 1979, has become the most abundant invasive plant along China's coast (Li et al., 2009). Such changes in species composition are known to alter soil C and N pools that subsequently alter GHG fluxes (Tong et al., 2018; Yuan et al., 2015). Our analysis strongly indicates that greater CH<sub>4</sub> fluxes and CO<sub>2</sub> emissions associated with the invasive *S. alterniflora* than with native species contribute to the risk of global warming (Fig. 2); however, its contribution to GHG fluxes shows a large spatial variation depending on wetland area and distribution in the coastal provinces of mainland China (Fig. S5; Table 3).

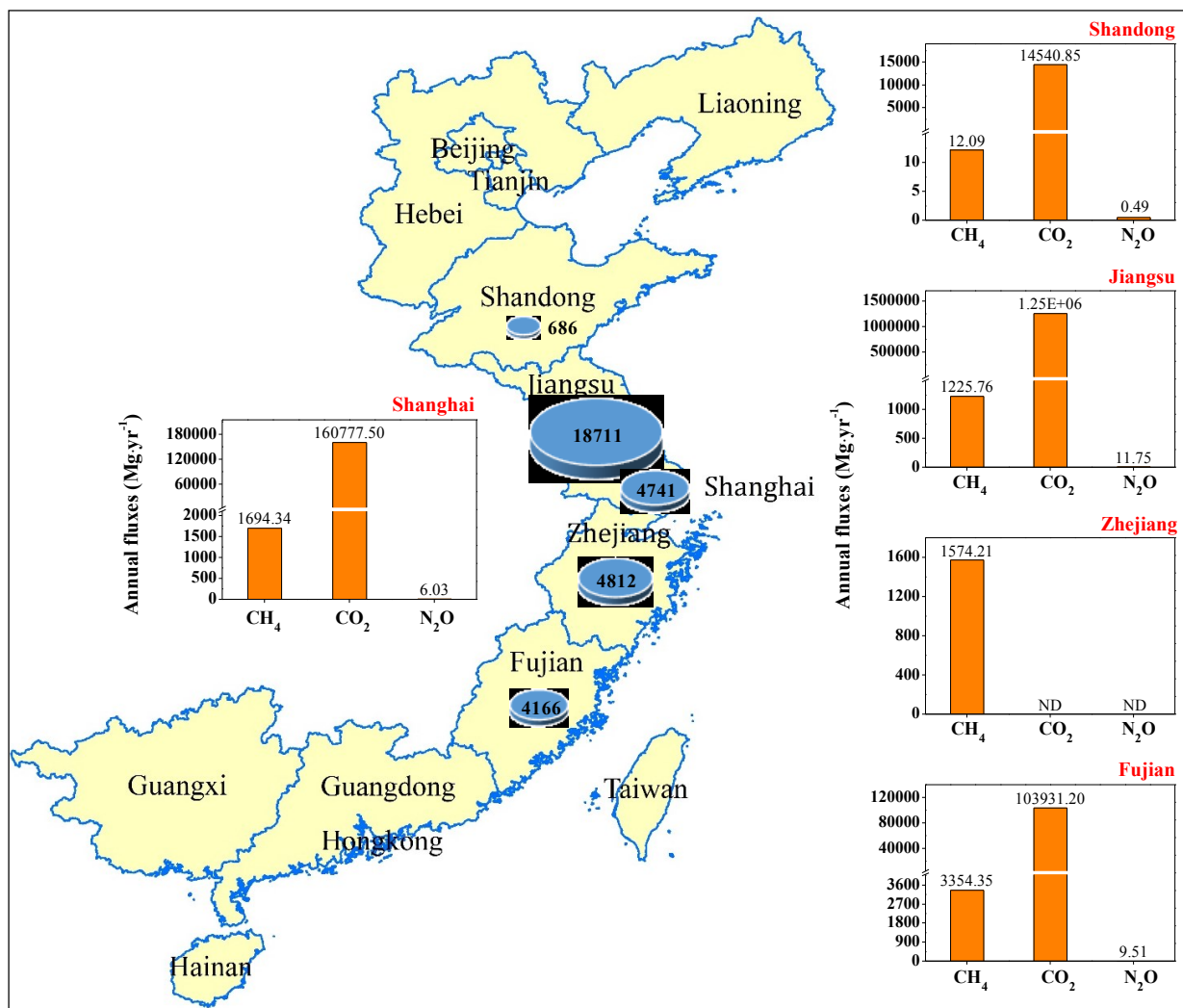


**Fig. S5** Total area (pie) and annual average GHG fluxes (histograms) of *Spartina alterniflora* from the coastal provinces of mainland China. *S. alterniflora* data were extracted from Zuo et al. (2012). ND: flux data were unavailable. Mg = 10<sup>3</sup> kg.

**Table 3** Total *S. alterniflora* area and GHG flux in each coastal province of China

Province	Area of <i>S. alterniflora</i> (ha)	Average GHG flux ( $\text{g}\cdot\text{m}^{-2}\cdot\text{y}^{-1}$ )			Total GHG flux ( $\text{Mg}\cdot\text{y}^{-1}$ )		
		CH <sub>4</sub>	CO <sub>2</sub>	N <sub>2</sub> O	CH <sub>4</sub>	CO <sub>2</sub>	N <sub>2</sub> O
Shandong	686	1.76	2119.66	0.07	12.09	14540.85	0.49
Jiangsu	18711	6.55	6704.90	0.06	1225.76	1254554.59	11.75
Shanghai	4741	35.74	3391.22	0.13	1694.34	160777.50	6.03
Zhejiang	4812	32.71	ND	ND	1574.21	ND	ND
Fujian	4166	80.52	2494.75	0.23	3354.35	103931.20	9.51
Overall	33116	31.46	3677.63	0.12	10417.18	1217884.29	40.50

The area of *S. alterniflora* were extracted from Zuo et al. (2012). ND: flux data were unavailable. Mg = 10<sup>3</sup> kg.

#### 4.3. Factors that affect the GHG fluxes across the coastal wetlands

GHG fluxes from wetland systems are highly spatially variable due to differences in climatic, soil, and environmental variables (Walter et al., 2015; Zhang et al., 2016). We first analyzed the effects of a single factor on CH<sub>4</sub>, CO<sub>2</sub>, and N<sub>2</sub>O fluxes for the coastal wetlands (Figs. S2-S4). The results showed that CH<sub>4</sub> fluxes increased with rising air temperature (Fig. S2a), which indicates that the CH<sub>4</sub> flux from coastal wetlands demonstrate an obvious influence of latitude. Increased air temperature accelerates the decomposition of organic matter which eventually supplies the substrate for CH<sub>4</sub> production, and also and enhances the activity of methanogens (Ding et al., 2004). CH<sub>4</sub> and CO<sub>2</sub> emissions generally increased with higher levels of soil moisture across the study sites, and N<sub>2</sub>O decreased with rising soil pH (Figs. S2-S4). Higher soil moisture is usually accompanied by anoxic environments that potentially limit organic C mineralization and CH<sub>4</sub> oxidation due to limited soil microbial respiration and decreases in methanotrophy (Hou et al., 2013; Hu et al., 2017). Low levels of soil pH tend to limit the assembly of functional N<sub>2</sub>O reductase and inhibit its reduction of N<sub>2</sub>O to N<sub>2</sub> during denitrification (Bakken et al., 2012; Zhou et al., 2017).

Our results also revealed a positive relationship between CO<sub>2</sub> fluxes and SOC associated with elevated levels of C substrate and nutrient availability, which may have led to greater release of C via regulation of plant and microbial activities directly or indirectly associated with C gas production and consumption

processes (Liu and Greaver, 2009). Except for the direct effects of the abovementioned factors, environmental parameters also affected GHG fluxes via interactions such as the indirect upregulation of CO<sub>2</sub> emissions by soil pH via its effect on SOC (path coefficient = 0.76; Fig. 4); multifactor interactions should thus be considered when exploring the controlling factors of GHG flux in coastal wetlands. Moreover, in our study, the changes in GHG fluxes with environmental parameters differed across climate zones (temperate vs subtropical; Figs. S2-S4); this revealed a potential control of temperature on the response of GHG fluxes to environmental parameters, which implies that a greater change in GHG fluxes will occur under warmer climatic conditions. For example, almost all environmental factors (e.g., air temperature, aboveground biomass, and SOC) are greater in subtropical zones than in temperate, and their impact on GHG fluxes is thus correspondingly greater (Figs. S2-S4). Note that, compared with CH<sub>4</sub> and CO<sub>2</sub>, no relationships between N<sub>2</sub>O fluxes and most environmental variables were detected (Fig. S4), possibly due to the combined effects of limited data availability and the complexity of interactions among the processes of nitrification and denitrification (Liu et al., 2014).

#### ***4.4. Implications and additional insights***

The synthesis presented here aimed to quantify the magnitude and patterns of fluxes of the three GHGs across the coastal wetlands of China. Overall, average CH<sub>4</sub> fluxes were lower than those reported from rice paddies, freshwater wetlands, and peatlands (Chen et al., 2013), and showed significant spatial differences. Based on an improved GWP evaluation method (Neubauer and Megonigal, 2015; Neubauer and Megonigal, 2019), our preliminary estimation found that, in China's coastal wetlands, the SGWP (10.78 Mg·CO<sub>2</sub>eq·ha<sup>-1</sup>·y<sup>-1</sup>) was approximately 30 times greater than the SGCP (0.38 Mg·CO<sub>2</sub>eq·ha<sup>-1</sup>·y<sup>-1</sup>; Table 1), which indicates that coastal wetlands represent a significant risk to increased global warming.

Major drivers of GHG emissions from coastal wetlands were a combination of biotic and abiotic factors,

which suggests that future effects of increases in temperature caused by global climate warming may exacerbate soil C losses in coastal systems. The results from this synthesis support the argument that plant species composition significantly impacts GHG flux due to variations in rates of primary productivity and nutrient use efficiency. Moreover, our data indicated that changes in tidal inundation within wetlands were drivers of CH<sub>4</sub> and CO<sub>2</sub> emissions, which highlights that future increases in tidal inundation and associated changes in soil/water salinity and sulfate caused by climate change-mediated rises in sea-level may promote and/or inhibit the C sequestration potential of coastal wetlands, which increases the uncertainty of estimates of GHG fluxes, especially in tidal wetlands. In summary, we found that two drivers of global change (increasing temperature and species invasion) might affect GHG fluxes from coastal wetlands in China and increase the risk of global warming by potentially increasing GHG emissions.

#### ***4.5. Limitations and future directions***

Although this study compiled and compared single studies, general conclusions about GHG fluxes across coastal wetlands may have inherent uncertainties due to site-specific environmental factors. Data limitations, especially of N<sub>2</sub>O fluxes compared with CH<sub>4</sub> and CO<sub>2</sub> emissions, makes precise estimation of fluxes in the three GHGs along wetland gradients and in contrasting wetland types problematic and weakens the explanatory power for N<sub>2</sub>O fluxes in coastal wetlands. The data used in this synthesis were biased toward the commonly used chamber-based methods of collecting and measuring gas fluxes, which may be inadequate for larger spatial-scale experiments (Pardo et al., 2015). Therefore, alternative techniques, such as eddy covariance techniques (Baldocchi, 2014), should be used to supplement data derived from chamber methods in larger spatial-scale studies. There was high heterogeneity in the dataset, including variation in sampling time, experimental duration, and vegetation type, which further increased the uncertainty of GHG estimates.

Consequently, our findings require validation using additional data from standardized, continuous field

observations from wetlands distributed across greater spatial and temporal ranges and scales to improve the quantification of spatiotemporal variation in GHG fluxes and the accurate assessment of the long-term net C balance. We suggest that the combined or interactive effects of invasive species and sea-level rise should be incorporated into future GHG measures and estimates to improve predictions of GHG fluxes and GWP in the context of global climate change. Moreover, plant productivity is an important factor that affects GHG effluxes. However, most of the articles we collected were about the data of the aboveground biomass, and there is very little data about belowground biomass or direct plant productivity. Therefore, future studies should focus on the influence of changes in these factors on GHG fluxes, and further research should be conducted on the C budget and the net ecosystem exchange of CO<sub>2</sub> in coastal wetlands. The results of our analysis will improve understanding of the main drivers and mechanisms of GHG fluxes between and within coastal wetlands; however, more detailed studies of spatiotemporal coupling and the key drivers that control GHG fluxes, such as tidal action and salt stress, are required.

## **5. Conclusions**

In summary, our analysis indicated that coastal wetland ecosystems have higher CO<sub>2</sub> but lower CH<sub>4</sub> emissions than inland and freshwater wetlands in China; further CH<sub>4</sub> and CO<sub>2</sub> effluxes decreased linearly with an increase of latitude. GHG fluxes were driven by a combination of climate, soil, and environmental factors, which suggests that future effects of increases in temperature caused by global climate warming may exacerbate soil C losses in coastal wetland systems. Our results found that plant species composition significantly impacts GHG flux and that coastal wetlands in China represent a significant risk to global change. Our data also indicated that future increases in tidal inundation and associated changes in soil/water salinity and sulfate caused by sea-level rise may promote and/or inhibit the C sequestration potential of coastal wetlands. This synthesized analysis improves understanding of the magnitude and spatial patterns of GHG

fluxes across coastal wetlands in China and highlights the urgent requirement to close existing knowledge gaps and elucidate spatiotemporal variations in long-term GHG fluxes in coastal wetland ecosystems at regional and global scales.

### **CRedit authorship contribution statement**

M.J.H. and C.T. conceived and designed the study; M.J.H. and X.Y.Y. performed the study and all statistical analyses; M.J.H. wrote the manuscript; and C.T., J.S, and J.P. assisted in interpreting the results and revising the manuscript. All authors reviewed the manuscript.

### **Declaration of competing interest**

The authors declare that they have no known competing financial interests or personal relationships that could have appeared to influence the work reported in this paper.

### **Acknowledgments**

This study was financially supported by the National Science Foundation of China (41801062, 41877335), the China Postdoctoral Science Foundation (2018M630731, 2019T120556), the Key Natural Science Foundation of Fujian Province (2019J02008), the Forestry Science and Technology Foundation of Fujian, a European Research Council Synergy grant (ERC-SyG-2013-610028 IMBALANCE-P), a Spanish Government grant (CGL2016-79835-P), and a Catalan Government grant (SGR 2017-1005). We sincerely thank Drs. Xiaohua Wan, Yi Li, Congting Ye, and Sheng Ding for their assistance with data analysis and the drawing of figures. Symbols in Fig. 7 are courtesy of the Integration and Application Network ([ian.umces.edu/symbols/](http://ian.umces.edu/symbols/)).

### **References**

Bakken, L.R., Bergaust, L., Liu, B.B., Frostegard, A., 2012. Regulation of denitrification at the cellular level: a clue to the understanding of N<sub>2</sub>O emissions from soils. *Philosophical Transactions of the Royal Society B: Biological Sciences* 367, 1226-1234.

- Baldocchi, D., 2014. Measuring fluxes of trace gases and energy between ecosystems and the atmosphere—the state and future of the eddy covariance method. *Global Change Biol.* 20, 3600-3609.
- Bartlett, K.B., Bartlett, D.S., Harriss, R.C., Sebacher, D.I., 1987. Methane emissions along a salt marsh salinity gradient. *Biogeochemistry* 4, 183-202.
- Bates, D., Machler, M., Bolker, B., Walker, S., 2018. *Fitting linear mixed-effects models using lme4*. arXiv:14065823.
- Bertness, M.D., 1991. Zonation of *Spartina patens* and *Spartina alterniflora* in New England salt marsh. *Ecology* 72, 138-148.
- Chambers, L.G., Osborne, T.Z., Reddy, R.K., 2013. Effect of salinity-altering pulsing events on soil organic carbon loss along an intertidal wetland gradient: a laboratory experiment. *Biogeochemistry* 115, 363-383.
- Chen, H., Zhu, Q.A., Peng, C.H., Wu, N., Wang, Y.F., Fang, X.Q., Jiang, H., Xiang, W.H., Chang, J., Deng, X.W., Yu, G.R., 2013. Methane emissions from rice paddies natural wetlands, lakes in China: synthesis new estimate. *Global Change Biol.* 19, 19-32.
- Chmura, G.L., 2013. What do we need to assess the sustainability of the tidal salt marsh carbon sink? *Ocean and Coastal Management* 83, 25-31.
- Collins, D.S., Avdis, A., Allison, P.A., Johnson, H.D., Hill, J., Piggott, M.D., Mha, H., Damit, A.R., 2017. Tidal dynamics and mangrove carbon sequestration during the Oligo-Miocene in the South China Sea. *Nat. Commun.* 8, 15698.
- Daniel, I., Degrandpre, M., Farías, L., 2013. Greenhouse gas emissions from the Tubul-Raqui estuary (central Chile 36°S). *Estuarine Coastal Shelf Science* 134, 31-44.
- Davidson, L.C., Cott, G.M., Devaney, J.L., Simkanin, C., 2018. Differential effects of biological invasions on coastal blue carbon: A global review and meta - analysis. *Global Change Biol.* 24, 5218–5230.
- Ding, W.X., Cai, Z.C., Tsuruta, H., 2004. Cultivation, nitrogen fertilization, and set-aside effects on methane uptake in a drained marsh soil in Northeast China. *Global Change Biol.* 10, 1801-1809.
- Eriksson, T., Öquist, M.G., Nilsson, M.B., 2010. Production and oxidation of methane in a boreal mire after a decade of increased temperature and nitrogen and sulfur deposition. *Global Change Biol.* 16, 2130-2144.
- Estop-Aragónés, C., Zajac, K., Blodau, C., 2016. Effects of extreme experimental drought and rewetting on CO<sub>2</sub> and CH<sub>4</sub> exchange in mesocosms of fourteen European peatlands with different nitrogen and sulfur deposition. *Global Change Biol.* 22, 2285-2300.
- Falkowski, P., Scholes, R.J., Boyle, E., Canadell, J., Canfield, D., Elser, J., Gruber, N., Hibbard, K., Hoegberg, P., Linder, S., 2000. The global carbon cycle: a test of our knowledge of earth as a system. *Science* 290, 291-296.
- Flury, S., McGinnis, D.F., Gessner, M.O., 2010. Methane emissions from a freshwater marsh in response to experimentally simulated global warming and nitrogen enrichment. *J. Geophys. Res.-Biogeo.* 115, 93-101.
- Gauci, V., Dise, N.B., Howell, G., Jenkins, M.E., 2015. Suppression of rice methane emission by sulfate deposition in simulated acid rain. *J. Geophys. Res.-Biogeo.* 113, 159-169.
- He, Y.H., Zhou, X.H., Jiang, L.L., Li, M., Du, Z.G., Zhou, G.Y., Shao, J.J., Wang, X.H., Xu, Z.H., Hosseini Bai, S., Wallace, H., Xu, C.Y., 2016. Effects of biochar application on soil greenhouse gas fluxes: a meta - analysis. *Global Change Biology Bioenergy* 9, 743–755.
- Holm, G.O., Perez, B.C., Mcwhorter, D.E., Krauss, K.W., Johnson, D.J., Raynie, R.C., Killebrew, C.J., 2016. Ecosystem level methane fluxes from tidal freshwater and brackish marshes of the Mississippi River Delta: Implications for coastal wetland carbon projects. *Wetlands* 36, 401-413.
- Hou, C.C., Song, C.C., Li, Y., Wang, J., Song, Y., Wang, X., 2013. Effects of water table changes on soil CO<sub>2</sub>, CH<sub>4</sub> and N<sub>2</sub>O fluxes during the growing season in freshwater marsh of Northeast China. *Environmental Earth Sciences* 69, 1963-1971.
- Hu, M.J., Peñuelas, J., Sardans, J., Sun, Z.G., Wilson, B.J., Huang, J.F., Zhu, Q.L., Tong, C., 2018. Stoichiometry patterns of plant organ N and P in coastal herbaceous wetlands along the East China Sea: implications for biogeochemical niche. *Plant Soil* 431, 273-288.

- Hu, M.J., Ren, H.C., Ren, P., Li, J.B., Wilson, B.J., Tong, C., 2017. Response of gaseous carbon emissions to low-level salinity increase in tidal marsh ecosystem of the Min River estuary, southeastern China. *J. Environ. Sci.* 52, 210-222.
- IPCC, 2007. *Climate Change 2007: The Scientific Basis*. Cambridge University Press, New York, USA.
- IPCC, 2013. *Climate Change 2013: The Physical Science Basis*. Cambridge University Press, Cambridge, United Kingdom and New York, NY, USA.
- IPCC, 2014. *Climate Change 2014: Synthesis Report. Contribution of Working Groups I, II and III to the Fifth Assessment Report of the Intergovernmental Panel on Climate Change Rep.* IPCC, Geneva, Switzerland, p. 151.
- IPCC, 2018. *Summary for Policymakers*. In: *Global warming of 1.5°C*. World Meteorological Organization, Geneva, Switzerland, 32 pp.
- Kirwan, M.L., Megonigal, J.P., 2013. Tidal wetland stability in the face of human impacts and sea-level rise. *Nature* 504, 53-60.
- Laanbroek, H.J., 2010. Methane emission from natural wetlands: interplay between emergent macrophytes and soil microbial processes. A mini-review. *Ann Bot* 105, 141-153.
- Li, B., Liao, C.Z., Zhang, X.D., Chen, H.L., Wang, Q., Chen, Z.Y., Gan, X.J., Wu, J.H., Zhao, B., Ma, Z.J., 2009. *Spartina alterniflora* invasions in the Yangtze River estuary, China: an overview of current status and ecosystem effects. *Ecol. Eng.* 35, 511-520.
- Li, Z., Tian, D., Wang, B., Wang, J., Wang, S., Chen, H.Y., Xu, X., Wang, C., He, N., Niu, S., 2019. Microbes drive global soil nitrogen mineralization and availability. *Global Change Biol.* 25, 1078-1088.
- Liu, C., Lu, M., Cui, J., Li, B., Fang, C.M., 2014. Effects of straw carbon input on carbon dynamics in agricultural soils: a meta-analysis. *Global Change Biol.* 20, 1366-1381.
- Liu, L.L., Greaver, T.L., 2009. A review of nitrogen enrichment effects on three biogenic GHGs: the CO<sub>2</sub> sink may be largely offset by stimulated N<sub>2</sub>O and CH<sub>4</sub> emission. *Ecol. Lett.* 12, 1103-1117.
- Lu, W.Z., Xiao, J.F., Liu, F., Zhang, Y., Liu, C.A., Lin, G.H., 2016. Contrasting ecosystem CO<sub>2</sub> fluxes of inland and coastal wetlands: a meta - analysis of eddy covariance data. *Global Change Biol.* 23, 1180-1198.
- Nahlik, A.M., Mitsch, W.J., 2011. Methane emissions from tropical freshwater wetlands located in different climatic zones of Costa Rica. *Global Change Biology* 17, 1321-1334.
- Nelson, D.W., Sommers, L.E., 1996. Total carbon, organic carbon and organic matter. D.L. Sparks (Ed.), *Methods of soil analysis. Part 3. Chemical Methods*. Soil Science Society of America, American Society of Agronomy, Madison, WI, pp. 961-1010.
- Neubauer, S.C., Megonigal, J.P., 2015. Moving beyond global Warming potentials to quantify the climatic role of ecosystems. *Ecosystems* 18, 1000-1013.
- Neubauer, S.C., Megonigal, J.P., 2019. Correction to: Moving Beyond Global Warming Potentials to Quantify the Climatic Role of Ecosystems. *Ecosystems*, <https://doi.org/10.1007/s10021-10019-00422-10025>.
- Niu, Z., Zhang, H., Wang, X., Yao, W., Zhou, D., Zhao, K., Zhao, H., Li, N., Huang, H., Li, C.J.C.S.B., 2012. Mapping wetland changes in China between 1978 and 2008. *Ecol. Appl.* 22, 2813-2823.
- O'Connell, C.S., Ruan, L.L., Silver, W.L., 2018. Drought drives rapid shifts in tropical rainforest soil biogeochemistry and greenhouse gas emissions. *Nat. Commun.* 9, 1348.
- Oberski, D.J.J.o.S.S., 2014. lavaan. survey: An R package for complex survey analysis of structural equation models. *Psychol. Methods* 19, 1-27.
- Olefeldt, D., Euskirchen, E.S., Harden, J., Kane, E., Mcguire, A.D., Waldrop, M.P., Turetsky, M.R., 2017. A decade of boreal rich fen greenhouse gas fluxes in response to natural and experimental water table variability. *Global Change Biol.* 23, 2428-2440.
- Pardo, G., Moral, R., Aguilera, E., Prado, A., 2015. Gaseous emissions from management of solid waste: a systematic review. *Global Change Biol.* 21, 1313-1327.
- Poffenbarger, H.J., Needelman, B.A., Megonigal, J.P., 2011. Salinity influence on methane emissions from tidal marshes. *Estuaries and Coasts* 34, 103-111.

Wetlands 31, 831-842.

- Purdy, K.J., Nedwell, D.B., Embley, T.M., 2003. Analysis of the sulfate-reducing bacterial and methanogenic archaeal populations in contrasting Antarctic sediments. *Appl. Environ. Microb.* 69, 3181-3191.
- Qiu, J.X., 2015. A global synthesis of the effects of biological invasions on greenhouse gas emissions. *Global Ecology Biogeography* 24, 1351-1362.
- R Development Core Team, 2020. R: A language and environment for statistical computing. R Foundation for Statistical Computing, Vienna, Austria. ISBN 3-900051-07-0, URL <http://www.R-project.org>.
- Segarra, K., E. A., Samarkin, V., King, E., Meile, C., Joye, S.B., 2013. Seasonal variations of methane fluxes from an unvegetated tidal;freshwater mudflat (Hammersmith Creek, GA). *Biogeochemistry* 115, 349-361.
- Sun, Z.G., Sun, W.L., Tong, C., Zeng, C.S., Yu, X., Mou, X.J., 2015. China's coastal wetlands: Conservation history, implementation efforts, existing issues and strategies for future improvement. *Environ Int* 79, 25-41.
- Tian, D., Xiang, Y., Wang, B., Li, M., Liu, Y., Wang, J., Li, Z., Niu, S., 2018. Cropland abandonment enhances soil inorganic nitrogen retention and carbon stock in China: A meta - analysis. *Land Degrad. Dev.* 29, 3898-3906.
- Tong, C., Morris, J.T., Huang, J.F., Xu, H., Wan, S.A., 2018. Changes in pore - water chemistry and methane emission following the invasion of *Spartina alterniflora* into an oligohaline marsh. *Limnol. Oceanogr.* 63, 384-396.
- Turetsky, M.R., Kotowska, A., Bubier, J., Dise, N.B., Crill, P., Hornibrook, E.R.C., Minkinen, K., Moore, T.R., Myers - Smith, I.H., Nykänen, H., 2014. A synthesis of methane emissions from 71 northern, temperate, and subtropical wetlands. *Global Change Biol.* 20, 2183-2197.
- Walter, K., Don, A., Fuss, R., Kern, J., Drewer, J., Flessa, H., 2015. Direct nitrous oxide emissions from oilseed rape cropping: a meta-analysis. *Global Change Biology Bioenergy* 7, 1260-1271.
- Wilson, B.J., Mortazavi, B., Kiene, R.P., 2015. Spatial and temporal variability in carbon dioxide and methane exchange at three coastal marshes along a salinity gradient in a northern Gulf of Mexico estuary. *Biogeochemistry* 123, 329-347.
- Xiao, D.R., Deng, L., Dong - Gill, K., Huang, C.B., Tian, K., 2019. Carbon budgets of wetland ecosystems in China. *Global Change Biol.*
- Xu, X.W.H., Zou, X.Q., Cao, L.G., Zhamangulova, N., Zhao, Y.F., Tang, D.H., Liu, D.W., 2014. Seasonal and spatial dynamics of greenhouse gas emissions under various vegetation covers in a coastal saline wetland in southeast China. *Ecol. Eng.* 73, 469-477.
- Yu, G.R., Zhu, X.J., Fu, Y.L., He, H.L., Wang, Q.F., Wen, X.F., Li, X.R., Zhang, L.M., Zhang, L., Su, W., 2013. Spatial patterns and climate drivers of carbon fluxes in terrestrial ecosystems of China. *Global Change Biol.* 19, 798-810.
- Yuan, J.J., Ding, W.X., Liu, D.Y., Kang, H., Freeman, C., Xiang, J., Lin, Y.X., 2015. Exotic *Spartina alterniflora* invasion alters ecosystem-atmosphere exchange of CH<sub>4</sub> and N<sub>2</sub>O and carbon sequestration in a coastal salt marsh in China. *Global Change Biol.* 21, 1567-1580.
- Zhang, B.W., Tian, H.Q., Wei, R., Bo, T., Lu, C.Q., Jia, Y., Banger, K., Pan, S.F., 2016. Methane emissions from global rice fields: Magnitude, spatiotemporal patterns, and environmental controls. *Global Biogeochem. Cy.* 30, 10.1002/2016GB005381.
- Zhao, X., Liu, S.L., Pu, C., Zhang, X.Q., Xue, J.F., Zhang, R., Wang, Y.Q., Lal, R., Zhang, H.L., Chen, F., 2016. Methane and nitrous oxide emissions under no-till farming in China: a meta-analysis. *Global Change Biol.* 22, 1372-1384.
- Zhou, C.H., Mao, Q.Y., Xiao, X.U., Fang, C.M., Luo, Y.M., Bo, L., 2016. Preliminary analysis of C sequestration potential of blue carbon ecosystems on Chinese coastal zone. *Sci Sin Vitae* 46, 475-486.
- Zhou, M.H., Zhu, B.O., Wang, S.J., Zhu, X.Y., Vereecken, H., 2017. Stimulation of N<sub>2</sub>O emission by manure application to agricultural soils may largely offset carbon benefits: a global meta-analysis. *Global Change Biol.* 23, 4068-4083.
- Zhu, X.D., Zhuang, Q.L., Qin, Z.C., Glagolev, M., Song, L.L., 2013. Estimating wetland methane emissions from the northern high latitudes from 1990 to 2009 using artificial neural networks. *Global Biogeochem. Cy.* 27, 592-604.
- Zuo, P., Zhao, S.H., Liu, C.A., Wang, C.H., Liang, Y.B., 2012. Distribution of *Spartina* spp. along China's coast. *Ecol.*

Eng. 40, 160-166.